Environmental Pollution 195 (2014) 39–47

Contents lists available at ScienceDirect

Environmental Pollution

journal homepage: www.elsevier.com/locate/envpol

On the use of an explicit chemical mechanism to dissect peroxy acetyl nitrate formation

Likun Xue [a, b, *], Tao Wang [a, b, c, *], Xinfeng Wang [b], Donald R. Blake [d], Jian Gao [c], Wei Nie [e], Rui Gao [b], Xiaomei Gao [b, f], Zheng Xu [b], Aijun Ding [e], Yu Huang [a], Shuncheng Lee [a], Yizhen Chen [c], Shulan Wang [c], Fahe Chai [c], Qingzhu Zhang [b], Wenxing Wang [b, c]

[a] Department of Civil and Environmental Engineering, Hong Kong Polytechnic University, Hong Kong, China
[b] Environment Research Institute, Shandong University, Ji'nan, Shandong, China
[c] Chinese Research Academy of Environmental Sciences, Beijing, China
[d] Department of Chemistry, University of California at Irvine, Irvine, CA, USA
[e] Institute for Climate and Global Change Research, Nanjing University, Nanjing, Jiangsu, China
[f] School of resources and environment, Ji'nan University, Shandong, China

ARTICLE INFO

Article history:
Received 2 June 2014
Received in revised form
3 August 2014
Accepted 7 August 2014
Available online 3 September 2014

Keywords:
Peroxy acetyl nitrate
Master Chemical Mechanism
OVOCs
Aromatics
Isoprene

ABSTRACT

Peroxy acetyl nitrate (PAN) is a key component of photochemical smog and plays an important role in atmospheric chemistry. Though it has been known that PAN is produced via reactions of nitrogen oxides (NO_x) with some volatile organic compounds (VOCs), it is difficult to quantify the contributions of individual precursor species. Here we use an explicit photochemical model – Master Chemical Mechanism (MCM) model – to dissect PAN formation and identify principal precursors, by analyzing measurements made in Beijing in summer 2008. PAN production was sensitive to both NO_x and VOCs. Isoprene was the predominant VOC precursor at suburb with biogenic impact, whilst anthropogenic hydrocarbons dominated at downtown. PAN production was attributable to a relatively small class of compounds including NO_x, xylenes, trimethylbenzenes, trans/cis-2-butenes, toluene, and propene. MCM can advance understanding of PAN photochemistry to a species level, and provide more relevant recommendations for mitigating photochemical pollution in large cities.

1. Introduction

Peroxy acetyl nitrate (PAN, $CH_3C(O)O_2NO_2$) is a key pollutant in photochemical smog. It is a cause of eye irritation and negatively affects vegetation, and is a potential mutagen for skin cancer (Stephens, 1969). Besides, it is an important player in atmospheric chemistry by acting as a reservoir of nitrogen oxides (NO_x). It is primarily formed in the industrialized/urbanized regions with abundant NO_x, and can be transported over long distances at low temperatures to remote regions and liberate NO_x (Singh et al., 1986). This process facilitates re-distribution of NO_x on regional (and even global) scales and controls ozone (O_3) production in both the source and downwind regions (LaFranchi et al., 2009). Consequently, investigating formation of PAN is an important part of understanding the formation of photochemical smog and assessing its impacts on human health and atmospheric chemistry.

In the troposphere, PAN is produced exclusively through photochemical reactions of volatile organic compounds (VOCs) in the presence of NO_x. Unlike O_3, precursors of PAN are only a relatively small set of VOCs that can generate peroxy acetyl radical ($CH_3C(O)O_2$, referred to from now on as PA, PA then combines with NO_2 to reversibly form PAN). PA comes directly from photolysis and $OH/NO_3/O_3$ oxidation of a small number of oxygenated VOCs (OVOCs) such as acetaldehyde, acetone, methacrolein (MACR), methyl vinyl ketone (MVK), methyl ethyl ketone (MEK) and methylglyoxal (MGLY). Besides some contribution from primary emissions (especially for acetaldehyde), most of these compounds are oxidation products (here referred to as second-generation precursors) of a certain class of hydrocarbons, *e.g.*, ethane, propene, isoprene, and some aromatics (hereafter referred to as first-generation precursors). The relative importance of individual precursors varies from place to place depending on the VOC composition (Liu et al., 2010; and references therein). Identification of the dominant precursors is key to effective control of PAN pollution.

Numerical models built on chemical mechanisms of different complexities are widely utilized to track out the PAN precursors.

* Corresponding authors.
E-mail addresses: xuelikun@gmail.com (L. Xue), cetwang@polyu.edu.hk (T. Wang).

http://dx.doi.org/10.1016/j.envpol.2014.08.005
0269-7491/

Roberts et al. (2001) developed a sequential reaction model that considers reactions of PANs and related aldehydes, and applied it to observations made in Nashville and Houston. LaFranchi et al. (2009) employed a steady state model containing chemistry of PANs, PA and related OVOCs to understand PAN formation in the Sacramento urban plumes. These models are capable of identifying the key 2nd-generation precursors (OVOCs), but cannot 'directly' link to the 1st-generation ones (hydrocarbons). Some studies adopted more comprehensive chemistry to explore the roles of 1st-generation PAN precursors (Grosjean et al., 2002; Liu et al., 2010), but the mechanisms they used were mostly compiled with a lumped approach (*e.g.*, the Statewide Air Pollution Research Center mechanism; usually abbreviated as SAPRC), from which the derived precursors were usually a class of hydrocarbons with similar structures/reactivities including non-PAN precursors. To our knowledge, there is lack of modeling studies that can determine the specific compounds of both generations of PAN precursors. Such information is critical for the PAN pollution control by identifying the responsible species and hence emission sources.

Here we demonstrate the application of the Master Chemical Mechanism (MCM) to better understand PAN photochemistry. MCM describes explicitly chemical degradations of individual hydrocarbon and OVOC species (Jenkin et al., 2003; Saunders et al., 2003), and hence facilitates a comprehensive evaluation of contributions from both generations of PAN precursors at a species level. In the present study, the MCM models are applied to intensive observations made both in downtown and at a downwind suburban site, to unravel formation of PAN and identify the major precursors in the atmosphere of Beijing.

2. Methodology

2.1. Field observations

Measurements were conducted in the Chinese Research Academy of Environmental Sciences (CRAES; 40°2′ N, 116°25′ E), a suburban site approximately 15 km north (normally downwind in summer) of city center (see Fig. 1). The site was located on the rooftop of a three-story building (~15 m above ground level). Surrounding our site there grows abundant fruit trees and landscape trees in the yard of CRAES. PAN, O_3, CO, NO, NO_2, NO_y, CH_4, non-methane hydrocarbons (NMHCs), carbonyls, aerosol size distribution and meteorological parameters were measured concurrently during 11 July–26 August 2008. In addition to the comprehensive observations at CRAES, whole air samples were taken along the 2nd and 3rd ring roads and in urban center (see also Fig. 1) for detection of hydrocarbons at downtown Beijing.

PAN was measured in real-time by a commercial analyzer (*Meteorologie Consult GmbH*), which detects PAN based on gas chromatographic (GC) separation followed by electron capture detection. This analyzer has a time resolution of 10 min, with a detection limit of 50 pptv, 2σ precision of 6% and uncertainty of 15%. During the campaign, the instrument baseline and sensitivity were calibrated weekly with a built-in calibration unit. Detailed information of this instrument and operation has been provided by J.M. Zhang et al. (2009) and Xue et al. (2011b).

CH_4 and C_2–C_{10} NMHCs were measured by collecting whole air samples in evacuated 2-L stainless-steel canisters followed by laboratory analyses. At CRAES, samples were taken every day with at least one sample in the afternoon (12:00–17:00 LT) on clean days and up to seven samples throughout the daytime (07:00–19:00 LT) on episode days (Wang et al., 2010b). The sampling frequency was 2 h and sampling duration was 2 min. A total of 130 samples were collected during the measurement period. At urban center, 18 samples were taken during the morning rush hours (07:00–09:00 LT) on 14 and 23 August 2008. After the campaign, the canisters were shipped to the University of California at Irvine for analyses by using a five-column multiple GC system coupled with flame ionization detection, electron capture detection and mass spectrometer detection (Simpson et al., 2010; Xue et al., 2011a; 2013b).

C_1–C_8 carbonyls were measured by collecting air samples in sorbent cartridges coated by *2,4*-dinitrophenylhydrazine (DNPH) equipped with an O_3 scrubber. The samples were taken generally every 2 h from 07:00 to 19:00 LT on selected O_3 episode days, with a sampling duration of 2 h for each sample and a flow rate of 1 L per minute. A total of 98 samples were collected at CRAES during the campaign. The collected samples were then eluted with acetonitrile and analyzed by a high-pressure liquid chromatography (*PerkinElmer, Series 2000*) in the laboratory of the Hong Kong Polytechnic University (Ho et al., 2011; Ho and Yu, 2004). Seventeen carbonyl species were detected, and only the data of acetaldehyde, acetone, MEK (mainly PAN precursors) and formaldehyde were used in the present study.

Ozone was measured by a commercial UV photometric analyzer (*TEI Model 49i*). CO was detected with a non-dispersive infrared analyzer (*API Model 300EU*). NO and NO_2 were observed with a chemiluminescence instrument (*TEI Model 42i*) equipped with a blue light converter (*Meteorologie consult GmbH*; Xu et al., 2013). NO_y was analyzed by another chemiluminescence analyzer (*TEI, Model 42cy*) with an externally placed molybdenum oxide converter. Particle number and size distributions (10 nm–10 μm) were measured in real-time by a wide-range particle spectrometer (*MSP, WPS model 1000XP*; Gao et al., 2012). Ambient temperature, pressure, relative humidity (RH), solar radiation and winds were monitored by a weather station. All these techniques and quality assurance and control procedures have been described elsewhere (Wang et al., 2010b; Xue et al., 2011b; J.M. Zhang et al., 2009).

2.2. The Master Chemical Mechanism models

Two sets of photochemical box models were set up to evaluate formation of PAN and its sensitivity to precursors at CRAES and in urban plumes. The model frameworks were largely similar to that described in our previous studies (Xue et al., 2013a, 2013b). Briefly, they were built on the latest version of MCM (*v3.2*) that explicitly describes degradation of 143 primary VOCs together with the latest IUPAC

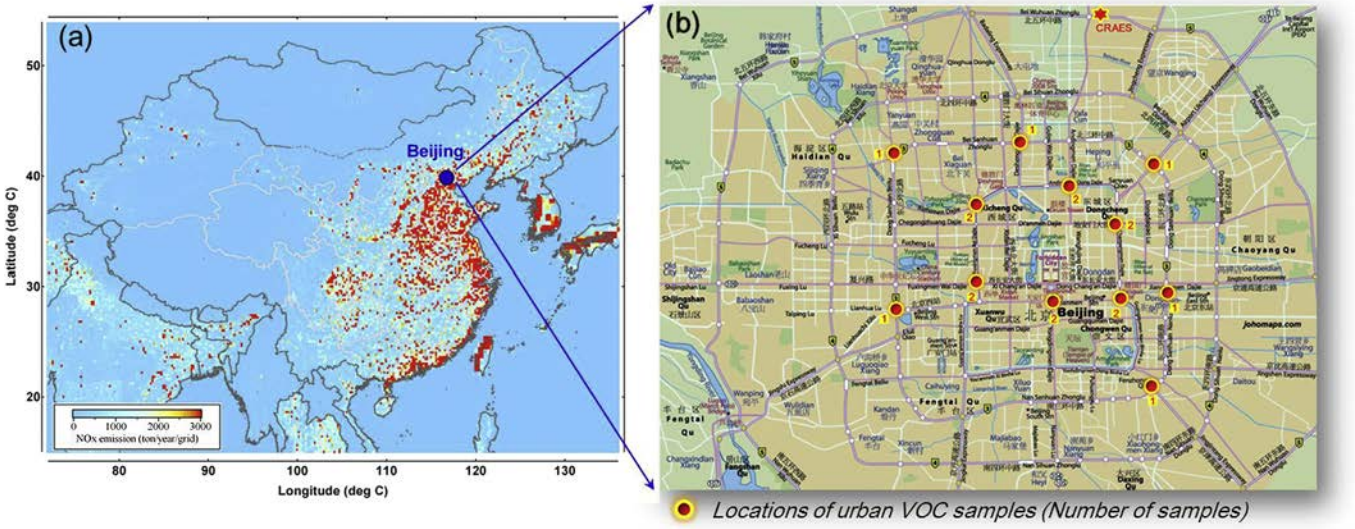

Fig. 1. (a) Map showing the study area and anthropogenic NO_x emissions (Q. Zhang et al., 2009) and (b) Locations of the CRAES site and urban VOC samples.

Table 1
Initial condition of the Urban Plume Model.[a]

	Measurement data[b]			Estimated data[c]	
CO	2.22 ppm	*cis-2*-pentene	358	NO	7.0 ppb
CH_4	2.64 ppm	*trans-2*-pentene	739	NO_2	35.8 ppb
C_2H_6	6670	*3*-Methyl-*1*-butene	169	O_3	28 ppb
C_3H_8	2740	*2*-Methyl-*1*-butene	669	PAN	0.72 ppb
n-Butane	3060	*2*-Methyl-*2*-butene	1080	SO_2	18.3 ppb
i-Butane	3020	*1,3*-Butadiene	580	HCHO	17.8 ppb
n-Pentane	2020	*1*-Pentene	304	CH_3CHO	8.44 ppb
i-Pentane	7590	Isoprene	766	acetone	12.0 ppb
n-Hexane	1170	*α*-Pinene	56	MEK	1.38 ppb
2-Methylpentane	2130	*β*-Pinene	9	H_2O	0.023%/%
3-Methylpentane	1360	C_2H_2	8850	Temp	298 K
2-Methylhexane	699	Benzene	3400	Pressure	751 mm Hg
3-Methylhexane	784	Toluene	5280		
2,2-Dimethylbutane	280	*o*-Xylene	903		
2,3-Dimethylbutane	996	*m,p*-Xylene	2550		
n-Heptane	1400	Ethylbenzene	1060		
n-Octane	344	Propylbenzene	139		
n-Nonane	114	*i*-Propylbenzene	56		
cyclohexane	120	*1,2,3*-Trimethylbenzene	217		
C_2H_4	12800	*1,2,4*-Trimethylbenzene	869		
C_3H_6	2510	*1,3,5*-Trimethylbenzene	212		
1-Butene	1210	*o*-ethyltoluene	198		
Methyl propene	1290	*m*-ethyltoluene	539		
cis-2-butene	795	*p*-ethyltoluene	261		
trans-2-butene	932	Styrene	192		

[a] The unit is pptv otherwise specified.
[b] The measurement data are average concentrations of the urban VOC samples.
[c] For O_3 and PAN, the average data at 08:00 LT at CRAES were used. For NO_x, SO_2 and carbonyls, the data were estimated from their regression against CO at CRAES and the urban CO data. For temperature, pressure and water content, the measured diurnal profiles at CRAES were used to constrain the model.

inorganic reactions (Jenkin et al., 2003; Saunders et al., 2003). Besides, heterogeneous loss of HO_2 on aerosols and nitrous acid formation via reactions of NO_2 on ground and aerosol surfaces were incorporated (Xue et al., 2013a). In addition to chemistry, physical processes including dry deposition and atmospheric dilution within the changing planetary boundary layer (PBL; is assumed to increase from 300 m at dawn to 1500 m at 14:00 local time and then decrease to 300 m at dusk) were also taken into account. Dry deposition velocities of PAN and other species were adopted from Zhang et al. (2003). Sensitivity studies with half or double deposition velocities for all species suggest an uncertainty of <15.6% in the model-calculated daytime PAN production rates. Photolysis frequencies were calculated within the model as a function of solar zenith angle, and were rescaled with the measured solar radiation (Xue et al., 2013a).

An observation-based model (OBM) was applied to the comprehensive data collected at CRAES. The observation data of O_3, CO, NO, NO_2, PAN, H_2O, temperature, pressure, CH_4, C_2–C_{10} NMHCs and carbonyls were averaged or interpolated into 1-*h* intervals and then prescribed to the model. Aerosol surface area and area-weighted radius were calculated based on the measured particle size and count and also used as model inputs (Gao et al., 2012). The model was run for selected photochemical episodes with 00:00 LT as initial time. During the simulations, the model was pre-run for nine days with constraints of the campaign-average data so that it reached a steady state for the unmeasured species (*e.g.*, radicals). The model output of the 10th day was used for analysis.

The *in-situ* net production rates of PAN + PA were computed every hour by the OBM. PAN and PA were considered as a couple in view of the high temperature during our study period (actually PA only accounts for a very minor fraction). In the troposphere, PA is formed through a huge number of reactions. In the present study, all of these reactions (*i.e.,* several hundred in the MCM) were tracked and grouped into a small number of formation pathways, namely, reactions involving acetaldehyde, acetone, MACR, MVK, MGLY, other OVOCs, reactions of O_3 + isoprene (*direct effect*) and O_3 + MPAN, and propagation of other radicals to PA. The production rate of PAN + PA can be estimated as the sum of these reaction rates. Loss of PAN + PA was mainly facilitated by reactions of PA with NO, HO_2, RO_2 and NO_3 as well as reactions of PAN + OH. The net rate can be determined as the difference between both.

Another box model was utilized to simulate formation of PAN in urban plumes of Beijing (hereafter referred to as Urban Plume Model; UPM). The UPM was initialized by the average concentrations of CO, CH_4, and C_2–C_{10} NMHC species measured at urban center and of O_3 and PAN at 08:00 LT at CRAES. For NO, NO_2 and carbonyls which were not measured in urban Beijing, the initial concentrations were estimated from their regression relationships with CO derived at CRAES (assuming that it was the same to those in urban Beijing) and the urban CO levels. Average diurnal variations of temperature, pressure, H_2O and solar radiation observed at CRAES were used to constrain the model. The initial conditions prescribed to the UPM are summarized in Table 1. The UPM was run for a 24-h period with 08:00 LT as initial time. Similarly, the model was run for ten times (reinitialized every 24-h with the same conditions) to stabilize the unassigned species (*e.g.*, radicals), and the output of the 10th day was analyzed.

3. Results and discussion

3.1. Characteristics of PAN and precursors

The measured data of PAN, related trace gases and meteorological parameters at CRAES over 11 July–26 August 2008 are documented in Fig. 2. Substantial photochemical air pollution remarked by elevated concentrations of PAN (O_3 as well) is illustrated. Throughout the 47-days campaign, 24 days (*i.e.*, 50%) were observed with 10-min concentrations of PAN exceeding 2 ppbv, and 10 days (21%) were noticed with the peak PAN over 4 ppbv. Two multi-day photochemical smog events were encountered during 22–25 July and 3–6 August 2008. The maximum concentration was recorded at 9.34 ppbv (10-min data) in the afternoon of 24 July 2008. Such level of PAN is comparable to those measured at an urban site (Peking University) of Beijing, *i.e.*, ~9.5 ppbv in summer 2006 (Shao et al., 2009) and ~14 ppbv in summer 2007 (Liu et al., 2010), and also among the highest records in polluted areas in recent decades, *e.g.*, 9.12 ppbv in Lanzhou, western China (J.M. Zhang et al., 2009), 3.9 ppbv downwind of Guangzhou, southern China (Wang et al., 2010a), 2.5 ppbv in Nashville, U.S. (Roberts et al., 2002); 6.5 ppbv in Houston, U.S. (Roberts et al., 2003), ~8 ppbv in Mexico City, Mexico (in 2003; Marley et al., 2007), 6.67 ppbv in Porto Alegre, Brazil (Grosjean et al., 2002), and ~10 ppbv (of PANs) in Tokyo, Japan (Kondo et al., 2008). These observations confirm the severe photochemical air pollution in summer in Beijing.

The average diurnal variations of PAN, O_3, NO_x, NO_y and temperature at CRAES are shown in Fig. 3. NO_x and NO_y showed double peaks in both early morning and evening, corresponding to the traffic rush hours, and a trough in the afternoon, mainly owing to

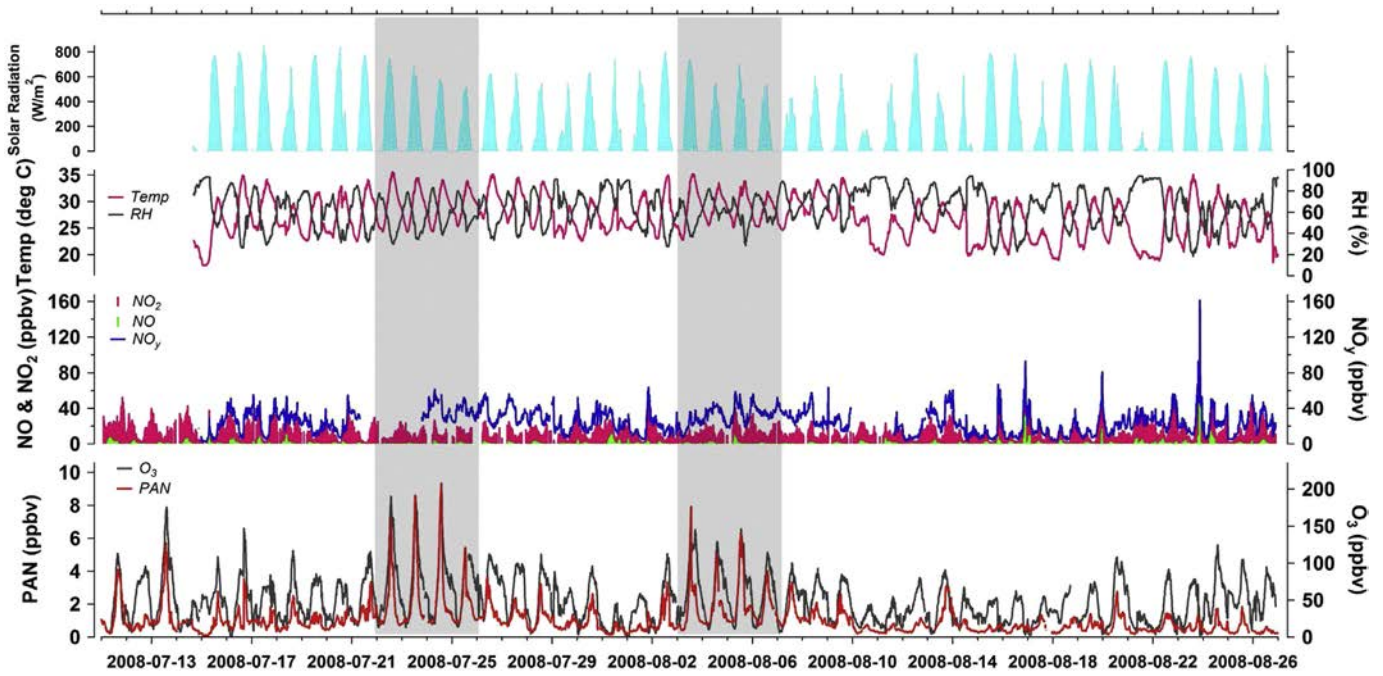

Fig. 2. Time series of trace gases and meteorological parameters observed at CRAES during 11 July–26 August 2008. The shaded areas correspond to the two multi-day photochemical episodes, which were subject to the detailed modeling analysis.

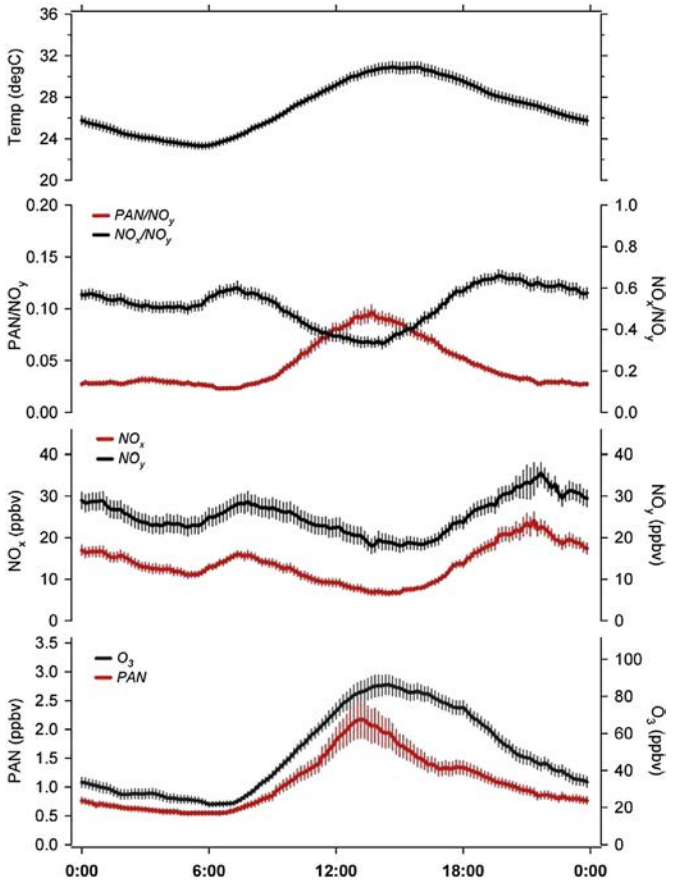

Fig. 3. Average diurnal variations of PAN, O_3, NO_x, NO_y, PAN/NO_y, NO_x/NO_y and temperature at CRAES during 11 July–26 August 2008. Error bars are standard errors.

evolution of PBL. PAN and O_3 exhibited typical photochemically-driven diurnal profiles with elevated levels in the afternoon. For PAN, it clearly accumulated in the morning, reached the maximum in early afternoon, and then decreased till the next morning. The sharp decrease in the afternoon should be result of thermal decomposition of PAN at high temperatures. Also shown in the figure are mean ratios of NO_x/NO_y and PAN/NO_y, which provide insights into the NO_y budget. At CRAES, NO_x accounted for approximately half of NO_y on average, with higher ratios (~60%) during the night-early morning period and lower values (33%) in the afternoon when the most intense photochemistry occurs. In comparison, PAN only composed a small fraction of NO_y with mean and afternoon ratios of 5% and 10% respectively. The highest PAN/NO_y ratio was determined at 25% during the heaviest episode (24 July) when the maximum PAN level was detected. Such PAN/NO_y ratios are comparable to or slightly smaller than those observed in Lanzhou (daytime-average and maximum of ~12% and ~50%; J.M. Zhang et al., 2009), Nashville (daytime-average and maximum of ~10% and ~27% for PANs/NO_y; Roberts et al., 2002), and Porto Alegre (daytime-average and maximum of ~11% and ~58%; Grosjean et al., 2002).

Fig. 4 shows the measured levels of hydrocarbons and OVOCs of interest at CRAES. These species are selected because they are the identified PAN precursors in the present study (see details in Section 3.3). In general, the observations indicate relatively high abundances of PAN precursors at this suburban site. The average concentrations (±SD) of acetaldehyde, acetone and MEK were 5.58 (±2.23), 7.23 (±2.97) and 0.71 (±0.35) ppbv, respectively. In terms of the first-generation precursors, toluene and isoprene were the most abundant species with mean levels of 1.68 (±1.55) and 1.57 (±1.27) ppbv, while propene, trans/cis-2-butenes, xylenes and trimethylbenzenes were in the magnitude of hundreds of pptv. A remarkable feature is the highly elevated levels of isoprene, indicating strong impact of biogenic VOC emissions at CRAES. Another feature to note is that the aromatic precursors were generally more abundant than the alkenes precursors.

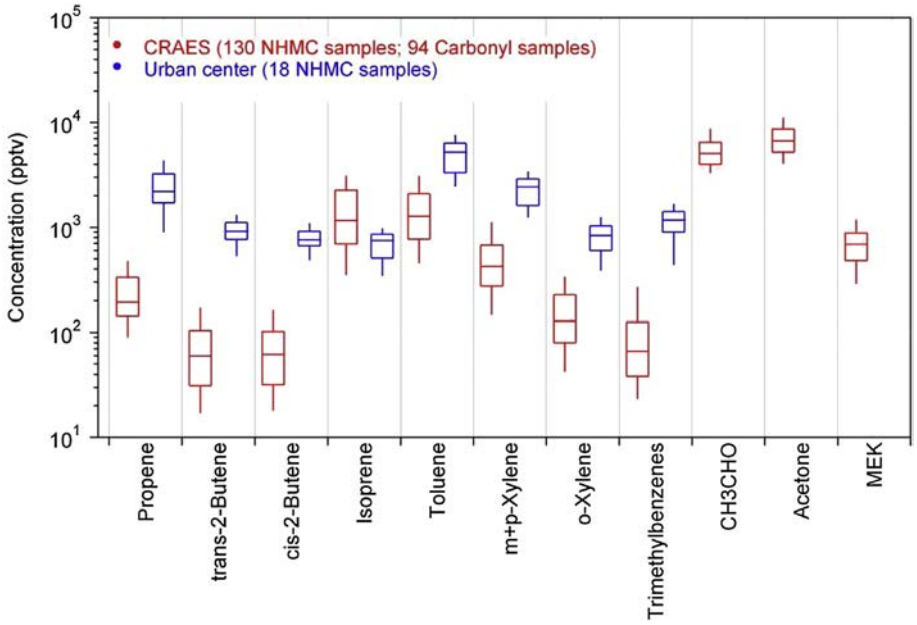

Fig. 4. Distributions of major PAN precursors observed at CRAES and urban center. The chart provides the 10th, 25th, 50th, 75th and 90th percentiles of the data. Note that carbonyls were only measured at CRAES.

Also shown in Fig. 4 are the hydrocarbon measurements taken at urban center. Except for isoprene, as was expected, the levels of PAN precursors at downtown were much higher (*i.e.*, 3–10 folders) than those at CRAES. Aromatic compounds were more abundant than the alkenes precursors, which is consistent with the case at CRAES. Overall, these observations demonstrate strong potential of PAN formation in the urban plumes of Beijing.

3.2. In-situ formation of PAN at CRAES

To understand the causes of elevated PAN concentrations at CRAES, we evaluated *in-situ* PAN production by the OBM and assessed its contribution to the measured levels during eight episode days (*i.e.*, 22–25 July and 3–6 August 2008). We estimated the amounts of PAN formed by *in-situ* photochemistry and compared them with the observed PAN accumulations. The observed accumulations were calculated as difference between the peak and early-morning concentrations of PAN, and the *in-situ* produced amounts were computed by integrating the OBM-calculated net rates over the course of PAN increase (note that such calculated amounts actually correspond to the production of PAN + PA, but they can represent approximately PAN as PA only accounts for a very small fraction). The comparison results are provided in Fig. 5.

Two types of episodes are noteworthy. On some cases, *i.e.*, 22, 23, 24 July and 3 August, *in-situ* production only accounted for 27% ~45% of the observed PAN accumulations. The discrepancy may arise from a transport source or a chemical source that is missed by

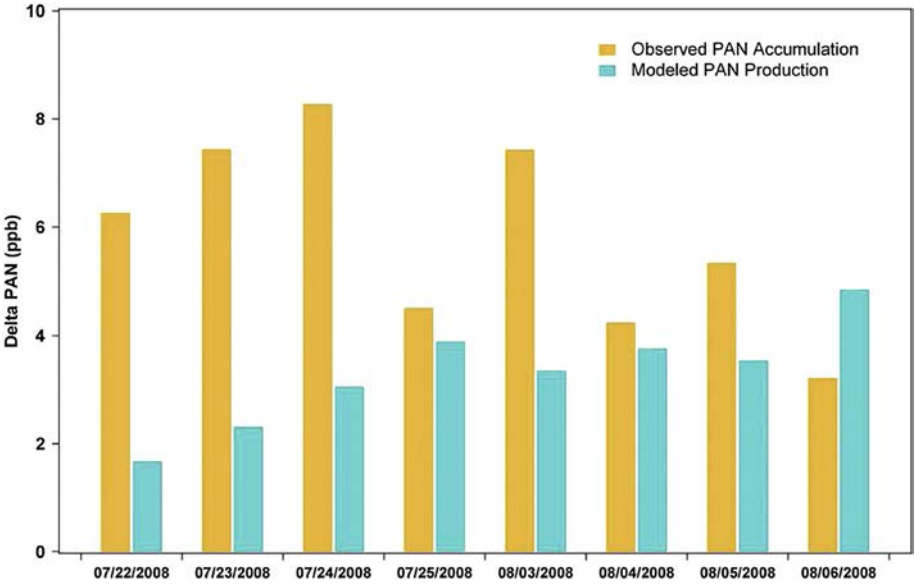

Fig. 5. Comparison of the OBM-estimated PAN production with the observed PAN accumulations during episodes at CRAES.

the MCM model. To find the reason, we examined day-to-day variations in the measurement data and found evidence from surface wind. During the PAN accumulation on days with model underprediction, a consistent surface wind pattern with northeasterly winds in early morning gradually switching to southeasterly winds around noon was noticed (figures not shown). In particular, the southerly winds around noontime correspond to the sharpest PAN increase. To the south of study site is located wide urban areas of Beijing. Thus transport of urban plumes should be responsible (or at least a very important factor) for the observed PAN accumulation. On the other episodes (*e.g.*, 25 July and 4 August), *in-situ* production explained majority (*i.e.*, 66%~100%) of the observed accumulations, indicating dominant role of local formation. On these episodes, surface winds were relatively weak and mostly northerly throughout the PAN accumulation from early morning to noon (actually the attack of southerly winds was delayed to late afternoon). These results illustrate important contributions from both *in-situ* chemistry and urban plume transport to the photochemical pollution at downwind suburban areas.

We further explored the major formation pathways of PA radical (and hence PAN) at CRAES. Fig. 6a shows the average contributions to PA production rates from individual grouped pathways during the episodes. Reactions of acetaldehyde (*i.e.*, oxidation by OH and NO_3) and MGLY (*i.e.*, photolysis and oxidation by OH and NO_3) are the most significant sources of PA, accounting for 34.1% (±2.0%; SD) and 30.3% (±1.6%) of the total production rate. Reactions (photolysis and oxidation by OH, NO_3 and O_3) of other OVOCs (except acetaldehyde, MGLY, MVK, MACR and acetone) and propagation of other radicals to PA (mainly including decomposition of some RO radicals and reactions of some higher acyl peroxy radicals with NO) are also important sources, with average contributions of 14.0% (±0.4%) and 19.6% (±1.0%) respectively. Other pathways such as reactions of acetone, MVK, MACR, O_3 + isoprene and O_3 + MPAN only represent a minor contribution (~2% in total). Acetaldehyde has both primary and secondary sources, and our modeling simulation suggests that more than half of the acetaldehyde was of photochemical origin at CRAES (see Section 3.3). The other OVOCs are mainly oxidation products of hydrocarbons. Thus it is important to further identify the first-generation precursors of PAN, which will be discussed in the next section. It's also noteworthy that a similar pattern of PA formation budget is obtained at urban center despite higher contribution from acetaldehyde (see Fig. 6b).

It should be noted that the isoprene photochemistry contributes to PA formation in a very complex manner. In the troposphere, degradation of isoprene evolves in several steps accompanying PA production at each step. For instance, the O_3-initiated oxidation of isoprene first produces PA, MACR and MVK (first step); the formed MACR and MVK then undergo photolysis and O_3 oxidation reactions to yield PA as well as MGLY (second step); and MGLY can be subject to photolysis and oxidation by O_3 and NO_3 to produce PA too (third step). In the present study, the model-calculated PA production from the "O_3 + isoprene" pathway only corresponds to contribution of the first step, and reactions of MACR and MVK represent contributions of the second step. An accurate evaluation of the contribution from isoprene need take all of these processes into account, and it remains a challenge given the fact that MGLY is also formed through oxidation of other VOCs such as aromatics. In the next section, we adopt an indirect approach to estimate the role of isoprene by conducting sensitivity studies with reduced isoprene levels.

3.3. Identification of primary precursors

3.3.1. Key precursors at CRAES

To find out the key first-generation precursors governing PAN formation, sensitivity modeling analyses were conducted to examine the PAN and precursor relationships. We adopted a relative incremental reactivity (RIR) concept that is widely applied in the OBM study of ozone formation (Cardelino and Chameides, 1995). Here RIR is defined as the ratio of decrease in PAN production rates to decrease in precursor concentrations (*i.e.*, 20% reduction is used in the present study), and can be used as a proxy for the effect of a given precursor reduction on PAN formation. We performed a number of sensitivity model runs to estimate the RIR for NO_x, alkane, alkene and aromatic classes as well as all of the individual C_2–C_{10} hydrocarbon species. During these simulations (except for NO_x), the model was not constrained by the OVOC measurements considering that these first-generation precursors contribute to PAN production through formation of OVOCs.

Fig. 7 shows the average RIRs for major precursor groups and species during eight episodes at CRAES. Only the species with relatively high RIR is discussed here. Production of PAN is found to be sensitive to both NO_x (RIR = 0.62 ± 0.40) and VOCs, which is similar to the transition regime of O_3 production derived from an urban site by Liu et al. (2012). In terms of VOCs, isoprene shows the highest RIR (0.47 ± 0.15), indicating that *in-situ* formation of PAN at CRAES was highly sensitive to isoprene. This is in line with the elevated levels of isoprene resulting from local biogenic emissions.

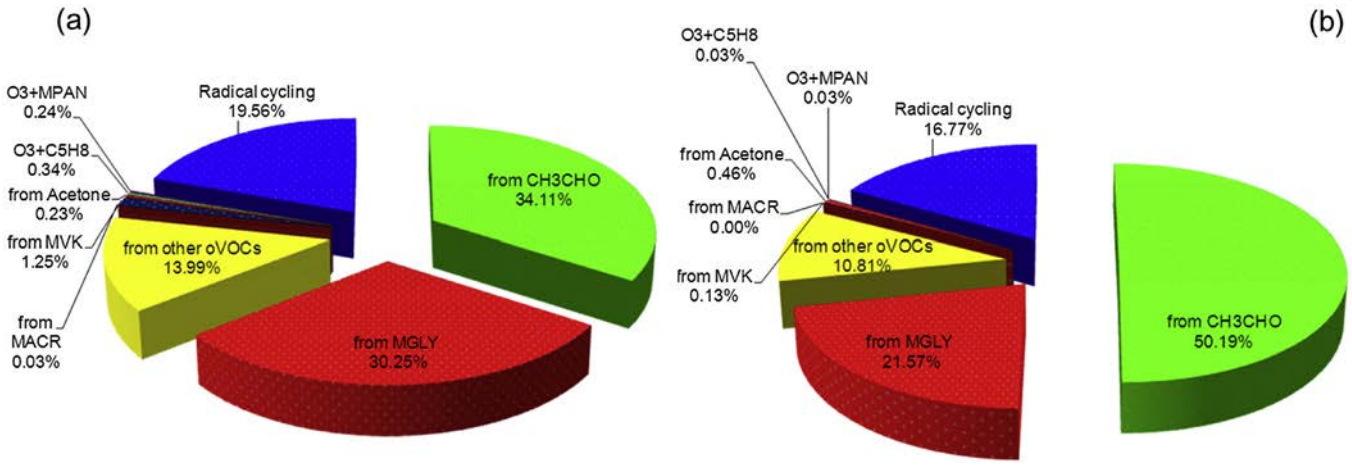

Fig. 6. Contributions of individual pathways to PA formation at (a) CRAES and (b) urban center. Radical cycling pathway refers to production of PA from decomposition of some RO radicals as well as reactions of some higher acyl peroxy radicals with NO (including over 100 reactions in the MCM *v3.2*).

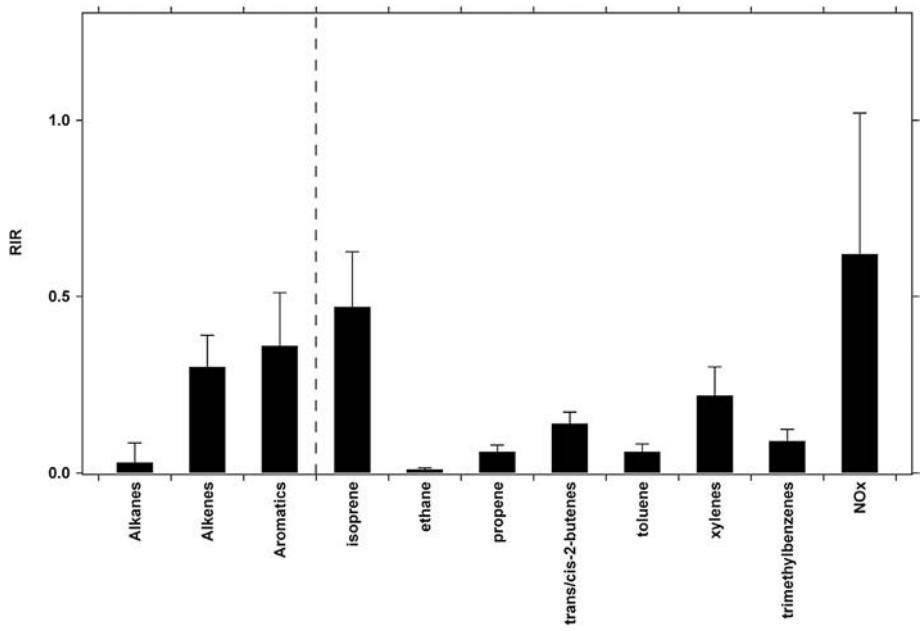

Fig. 7. Sensitivity of PAN production rate to major precursor groups and individual species at CRAES. Error bars are standard deviations.

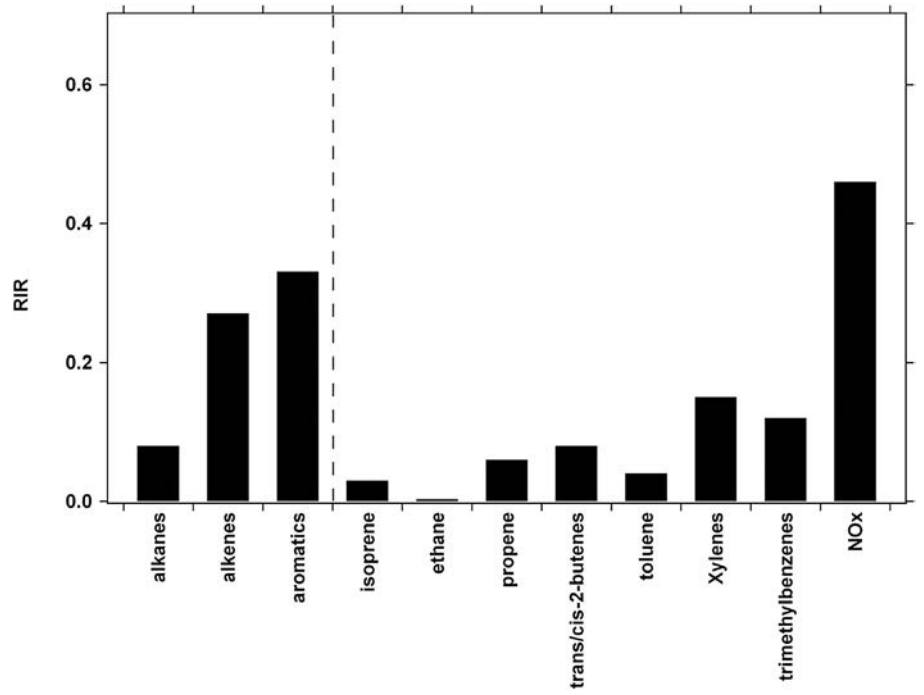

Fig. 8. Sensitivity of the modeled maximum PAN to major precursor groups and individual species in urban Beijing.

As to anthropogenic VOCs, aromatics (RIR = 0.36 ± 0.15) and alkenes (RIR = 0.30 ± 0.09) were the most significant first-generation PAN precursors. Moreover, we further identified the key species controlling PAN production. In fact, formation of PAN was only contributed by a small class of compounds. Specifically, NO_x, isoprene, xylenes, trans/cis-2-butenes, trimethylbenzenes, toluene and propene were the most important PAN precursors at CRAES, as evidence by their high positive RIRs.

We also assessed roughly the role of primary acetaldehyde in PAN formation. We conducted model runs with and without constraints of acetaldehyde and compared the PAN production rates between both cases, with a simple assumption that the scenario without constraints would produce only secondary acetaldehyde (it's noteworthy that our estimation of secondary acetaldehyde is only a lower limit, as our model cannot take into account the transported secondary acetaldehyde from upwind regions). The results show that the modeled 'secondary' acetaldehyde present a large fraction (57.2% ± 9.1%) of the measured levels, implying that the acetaldehyde was of both photochemical and primary origins at our suburban site. Without primary

acetaldehyde (here as an upper limit) taken into consideration, the daytime-average PAN production rates would be reduced by 21.6% (±6.4%) during the episodes (equivalent as an RIR value of 0.2). These results suggest the considerable role of primary acetaldehyde in photochemical formation of PAN in Beijing.

3.3.2. Key precursors in urban plume

The dominant primary precursors of PAN in urban Beijing were also determined with a similar approach but with the UPM, which was deployed to simulate chemical evolution of urban plumes released from downtown in early morning (see Section 2.2 for details). In the UPM analysis, RIR is defined as the ratio of decrease in the maximum PAN concentration to decrease in the precursor concentrations (note that the UPM cannot 'accurately' calculate the *in-situ* production rates of PAN without time-dependent constraints of measurements), and is used as a metric for the effect of an emission reduction on PAN concentrations. In the base run, the UPM-simulated peak PAN concentration was 7.92 ppbv, which is comparable to the maximum level observed at CRAES.

The UPM-estimated RIRs for major precursor groups and species are provided in Fig. 8. A similar transition regime of PAN production is derived with high RIR values for both NO_x and VOCs. The major difference from the result obtained at CRAES is the minor role of isoprene (RIR = 0.03) in the urban plume. This is within expectation in light of the extremely abundant anthropogenic hydrocarbons and relatively low concentrations of isoprene at the downtown area. Reactive aromatics (RIR = 0.33) turned out to be the most significant VOC precursor group in urban plume, while alkenes (RIR = 0.27) also played an important role. Furthermore, NO_x, xylenes, trimethylbenzenes, trans/cis-2-butenes, propene and toluene were identified as the key species contributing to PAN formation in urban plumes of Beijing. Such list of anthropogenic species is consistent with those determined at CRAES. Our results also agree with the previous study at an urban site that suggested aromatics as the dominant VOC precursor of PAN (Liu et al., 2010), but move forward to identify the responsible species.

Our analyses reveal that photochemical formation of PAN in the atmosphere of Beijing is attributable to a small number of precursors, namely, NO_x, xylenes, trans/cis-2-butenes, trimethylbenzenes, toluene and propene. These findings can support formulation of effective control strategies for mitigating photochemical smog. In Beijing, power plant, transportation and industry activities are recognized as the major anthropogenic emission sources of NO_x; paint usage, petrochemical industry and vehicle exhaust as major sources of xylenes and toluene; gasoline evaporation as predominant source of trans/cis-2-butenes; and vehicle exhaust as dominant source of propene (Liu et al., 2005; Song et al., 2007; Yuan et al., 2010). Therefore, it is recommended to cut emissions from these sectors in order to alleviate the PAN pollution in Beijing and hence reduce its harmful effect on human health and vegetation.

4. Conclusions

We analyzed measurements of PAN and PAN precursors made at a suburban site as well as hydrocarbon data collected at downtown Beijing. Severe photochemical air pollution was revealed with elevated levels of PAN up to 9.34 ppbv. *In-situ* photochemical production and transport of urban plumes were the processes contributing to PAN pollution at the study site. Highly elevated levels of PAN precursors were measured in urban atmospheres, suggesting strong potential of PAN formation in urban plumes of Beijing.

The MCM model is proved to be an ideal tool to understand photochemical formation of PAN and identify its key precursors (including NO_x, OVOCs and their parent hydrocarbons). In Beijing, the PAN production was sensitive to both NO_x and VOCs. At the suburban site impacted by biogenic emissions, isoprene was the most important VOC precursor, while anthropogenic VOCs dominated in urban plumes. Degradation of acetaldehyde, MGLY and other OVOCs as well as radical propagation reactions were the major formation pathways of PA radical and hence PAN. Photochemical formation of PAN can be attributed to NO_x and a small class of aromatic and olefin compounds, specifically xylenes, trans/cis-2-bentenes, trimethylbenzenes, propene and toluene. To mitigate the PAN pollution in Beijing, therefore, it is suggested to reduce the emissions from paint usage, vehicles, power plant, gasoline evaporation and petrochemical industry.

Acknowledgments

We appreciate Steven Poon, Pengju Xu, Yangchun Yu, Chao Yuan and Linlin Wang for their contribution to the field study, and thank *Drs.* Sarah and Steven Ho for their help in the laboratory analysis of OVOCs. We are grateful to the Master Chemical Mechanism group in University of Leeds for providing the mechanism. We also thank the anonymous reviewers who raised helpful comments to improve our original manuscript. The field measurements were funded by the National Basic Research Program (2005CB422203) and the central level scientific research institutes for basic R&D special fund business (Grant No. 2008KYYW01), and data analysis was supported by the Hong Kong Polytechnic University (1-BB94 and 1-ZV9N).

References

Cardelino, C.A., Chameides, W.L., 1995. An observation-based model for analyzing ozone precursor relationships in the urban atmosphere. J. Air Waste Manag. Assoc. 45, 161–180.

Gao, J., Chai, F.H., Wang, T., Wang, S.L., Wang, W.X., 2012. Particle number size distribution and new particle formation: new characteristics during the special pollution control period in Beijing. J. Environ. Sci. China 24, 14–21.

Grosjean, E., Grosjean, D., Woodhouse, L.F., Yang, Y.J., 2002. Peroxyacetyl nitrate and peroxypropionyl nitrate in Porto Alegre, Brazil. Atmos. Environ. 36, 2405–2419.

Ho, S.S.H., Ho, K.F., Liu, W.D., Lee, S.C., Dai, W.T., Cao, J.J., Ip, H.S.S., 2011. Unsuitability of using the DNPH-coated solid sorbent cartridge for determination of airborne unsaturated carbonyls. Atmos. Environ. 45, 261–265.

Ho, S.S.H., Yu, J.Z., 2004. Determination of airborne carbonyls: comparison of a thermal desorption/GC method with the standard DNPH/HPLC method. Environ. Sci. Technol. 38, 862–870.

Jenkin, M.E., Saunders, S.M., Wagner, V., Pilling, M.J., 2003. Protocol for the development of the Master Chemical Mechanism, MCM v3 (Part B): tropospheric degradation of aromatic volatile organic compounds. Atmos. Chem. Phys. 3, 181–193.

Kondo, Y., Morino, Y., Fukuda, M., Kanaya, Y., Miyazaki, Y., Takegawa, N., Tanimoto, H., McKenzie, R., Johnston, P., Blake, D.R., Murayama, T., Koike, M., 2008. Formation and transport of oxidized reactive nitrogen, ozone, and secondary organic aerosol in Tokyo. J. Geophys. Res. Atmos. 113.

LaFranchi, B.W., Wolfe, G.M., Thornton, J.A., Harrold, S.A., Browne, E.C., Min, K.E., Wooldridge, P.J., Gilman, J.B., Kuster, W.C., Goldan, P.D., de Gouw, J.A., Mckay, M., Goldstein, A.H., Ren, X., Mao, J., Cohen, R.C., 2009. Closing the peroxy acetyl nitrate budget: observations of acyl peroxy nitrates (PAN, PPN, and MPAN) during BEARPEX 2007. Atmos. Chem. Phys. 9, 7623–7641.

Liu, Y., Shao, M., Zhang, J., Fu, L.L., Lu, S.H., 2005. Distributions and source apportionment of ambient volatile organic compounds in Beijing city, China. J. Environ. Sci. Health Part A Toxic Hazard. Subst. Environ. Eng. 40, 1843–1860.

Liu, Z., Wang, Y.H., Gu, D.S., Zhao, C., Huey, L.G., Stickel, R., Liao, J., Shao, M., Zhu, T., Zeng, L.M., Liu, S.C., Chang, C.C., Amoroso, A., Costabile, F., 2010. Evidence of reactive aromatics as a major source of peroxy acetyl nitrate over China. Environ. Sci. Technol. 44, 7017–7022.

Liu, Z., Wang, Y., Gu, D., Zhao, C., Huey, L.G., Stickel, R., Liao, J., Shao, M., Zhu, T., Zeng, L., Amoroso, A., Costabile, F., Chang, C., Liu, S., 2012. Summertime photochemistry during CAREBeijing-2007: RO_x budgets and O_3 formation. Atmos. Chem. Phys. 12, 7737–7752.

Marley, N.A., Gaffney, J.S., Ramos-Villegas, R., Gonzalez, B.C., 2007. Comparison of measurements of peroxyacyl nitrates and primary carbonaceous aerosol concentrations in Mexico City determined in 1997 and 2003. Atmos. Chem. Phys. 7, 2277–2285.

Roberts, J.M., Flocke, F., Stroud, C.A., Hereid, D., Williams, E., Fehsenfeld, F., Brune, W., Martinez, M., Harder, H., 2002. Ground-based measurements of

peroxycarboxylic nitric anhydrides (PANs) during the 1999 Southern Oxidants Study Nashville Intensive. J. Geophys. Res. Atmos. 107.
Roberts, J.M., Jobson, B.T., Kuster, W., Goldan, P., Murphy, P., Williams, E., Frost, G., Riemer, D., Apel, E., Stroud, C., Wiedinmyer, C., Fehsenfeld, F., 2003. An examination of the chemistry of peroxycarboxylic nitric anhydrides and related volatile organic compounds during Texas Air Quality Study 2000 using ground-based measurements. J. Geophys. Res. Atmos. 108.
Roberts, J.M., Stroud, C.A., Jobson, B.T., Trainer, M., Hereid, D., Williams, E., Fehsenfeld, F., Brune, W., Martinez, M., Harder, H., 2001. Application of a sequential reaction model to PANs and aldehyde measurements in two urban areas. Geophys. Res. Lett. 28, 4583–4586.
Saunders, S.M., Jenkin, M.E., Derwent, R.G., Pilling, M.J., 2003. Protocol for the development of the Master Chemical Mechanism, MCM v3 (Part A): tropospheric degradation of non-aromatic volatile organic compounds. Atmos. Chem. Phys. 3, 161–180.
Shao, M., Lu, S.H., Liu, Y., Xie, X., Chang, C.C., Huang, S., Chen, Z.M., 2009. Volatile organic compounds measured in summer in Beijing and their role in ground-level ozone formation. J. Geophys. Res. Atmos. 114.
Simpson, I.J., Blake, N.J., Barletta, B., Diskin, G.S., Fuelberg, H.E., Gorham, K., Huey, L.G., Meinardi, S., Rowland, F.S., Vay, S.A., Weinheimer, A.J., Yang, M., Blake, D.R., 2010. Characterization of trace gases measured over Alberta oil sands mining operations: 76 speciated C_2–C_{10} volatile organic compounds (VOCs), CO_2, CH_4, CO, NO, NO_2, NO_y, O_3 and SO_2. Atmos. Chem. Phys. 10, 11931–11954.
Singh, H.B., Salas, L.J., Viezee, W., 1986. Global distribution of peroxyacetyl nitrate. Nature 321, 588–591.
Song, Y., Shao, M., Liu, Y., Lu, S.H., Kuster, W., Goldan, P., Xie, S.D., 2007. Source apportionment of ambient volatile organic compounds in Beijing. Environ. Sci. Technol. 41, 4348–4353.
Stephens, E.R., 1969. The formation, reactions and properties of peroxyacyl nitrates (PANs) in photochemical air pollution. Adv. Environ. Sci. Technol. 1, 119–146.
Wang, B., Shao, M., Roberts, J.M., Yang, G., Yang, F., Hu, M., Zeng, L.M., Zhang, Y.H., Zhang, J.B., 2010a. Ground-based on-line measurements of peroxyacetyl nitrate (PAN) and peroxypropionyl nitrate (PPN) in the Pearl River Delta, China. Int. J. Environ. Anal. Chem. 90, 548–559.
Wang, T., Nie, W., Gao, J., Xue, L.K., Gao, X.M., Wang, X.F., Qiu, J., Poon, C.N., Meinardi, S., Blake, D., Wang, S.L., Ding, A.J., Chai, F.H., Zhang, Q.Z., Wang, W.X., 2010b. Air quality during the 2008 Beijing Olympics: secondary pollutants and regional impact. Atmos. Chem. Phys. 10, 7603–7615.
Xu, Z., Wang, T., Xue, L.K., Louie, P.K.K., Luk, C.W.Y., Gao, J., Wang, S.L., Chai, F.H., Wang, W.X., 2013. Evaluating the uncertainties of thermal catalytic conversion in measuring atmospheric nitrogen dioxide at four differently polluted sites in China. Atmos. Environ. 76, 221–226.
Xue, L.K., Wang, T., Gao, J., Ding, A.J., Zhou, X.H., Blake, D.R., Wang, X.F., Saunders, S.M., Fan, S.J., Zuo, H.C., Zhang, Q.Z., Wang, W.X., 2013a. Ozone production in four major cities of China: sensitivity to ozone precursors and heterogeneous processes. Atmos. Chem. Phys. Discuss. 13, 27243–27285.
Xue, L.K., Wang, T., Guo, H., Blake, D.R., Tang, J., Zhang, X.C., Saunders, S.M., Wang, W.X., 2013b. Sources and photochemistry of volatile organic compounds in the remote atmosphere of western China: results from the Mt. Waliguan Observatory. Atmos. Chem. Phys. 13, 8551–8567.
Xue, L.K., Wang, T., Simpson, I.J., Ding, A.J., Gao, J., Blake, D.R., Wang, X.Z., Wang, W.X., Lei, H.C., Jing, D.Z., 2011a. Vertical distributions of non-methane hydrocarbons and halocarbons in the lower troposphere over northeast China. Atmos. Environ. 45, 6501–6509.
Xue, L.K., Wang, T., Zhang, J.M., Zhang, X.C., Deliger, Poon, C.N., Ding, A.J., Zhou, X.H., Wu, W.S., Tang, J., Zhang, Q.Z., Wang, W.X., 2011b. Source of surface ozone and reactive nitrogen speciation at Mount Waliguan in western China: new insights from the 2006 summer study. J. Geophys. Res. Atmos. 116.
Yuan, B., Shao, M., Lu, S.H., Wang, B., 2010. Source profiles of volatile organic compounds associated with solvent use in Beijing, China. Atmos. Environ. 44, 1919–1926.
Zhang, J.M., Wang, T., Ding, A.J., Zhou, X.H., Xue, L.K., Poon, C.N., Wu, W.S., Gao, J., Zuo, H.C., Chen, J.M., Zhang, X.C., Fan, S.J., 2009. Continuous measurement of peroxyacetyl nitrate (PAN) in suburban and remote areas of western China. Atmos. Environ. 43, 228–237.
Zhang, L., Brook, J.R., Vet, R., 2003. A revised parameterization for gaseous dry deposition in air-quality models. Atmos. Chem. Phys. 3, 2067–2082.
Zhang, Q., Streets, D.G., Carmichael, G.R., He, K.B., Huo, H., Kannari, A., Klimont, Z., Park, I.S., Reddy, S., Fu, J.S., Chen, D., Duan, L., Lei, Y., Wang, L.T., Yao, Z.L., 2009. Asian emissions in 2006 for the NASA INTEX-B mission. Atmos. Chem. Phys. 9, 5131–5153.